Title: Black Hole Mining Effect

Date: Nov 10, 2017 03:30 PM

URL: http://pirsa.org/17110101

Abstract:

Testing quantum effect (extra-dimension/BH mining effect) with pulsar-BH system

Yin-Zhe Ma

University of KwaZulu-Natal, South Africa

With Michael Kavic, Matthew Lippert, John Estes, John Simonetti

See also “Fundamental physics with SKA: Gravity and Gravitational radiation”

Astrophysical windows of quantum BH

- Accretion disk dynamics
- Accretion matter direct imaging
- Lensing distance objects
- Gravitational in-spirals (ringdown, echos)
- Binary pulsar--BH system

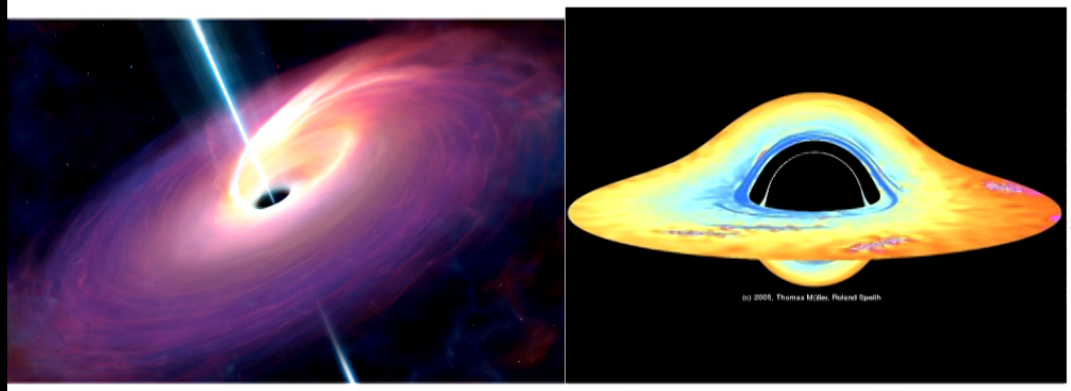

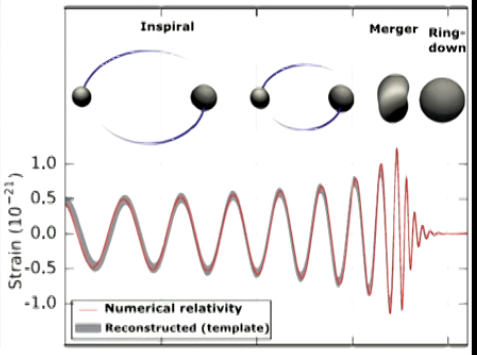

Giddings 2014; PRD, Pen & Broderick, 2014; MNRAS, Yunes, Yagi, Pretorius, 2016 PRD


Giddings 2014; PRD,
CAUTION

The most accurate clock--- Pulsars

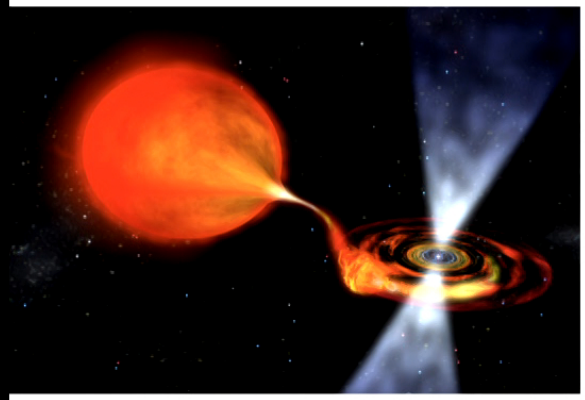

The Relativistic Binary Pulsar B1913+16: Thirty Years of Observations and Analysis

Joel M. Weisberg

Dept. of Physics & Astronomy, Carleton College, Northfield, MN

Joseph H. Taylor

Dept. of Physics, Princeton University, Princeton, NJ

Abstract. We describe results derived from thirty years of observations of PSR B1913+16. Together with the Keplerian orbital parameters, measurements of the relativistic periastron advance and a combination of gravitational redshift and time dilation yield the stellar masses with high accuracy. The measured rate of change of orbital period agrees with that expected from the emission of gravitational radiation, according to general relativity, to within about 0.2 percent. Systematic effects depending on the pulsar distance and on poorly known Galactic constants now dominate the error budget, so tighter bounds will be difficult to obtain. Geodetic precession of the pulsar spin axis leads to secular changes in pulse shape as the pulsar-observer geometry changes. This effect makes it possible to model the two-dimensional structure of the beam. We find that the beam is elongated in the latitude direction and appears to be pinched in longitude near its center.

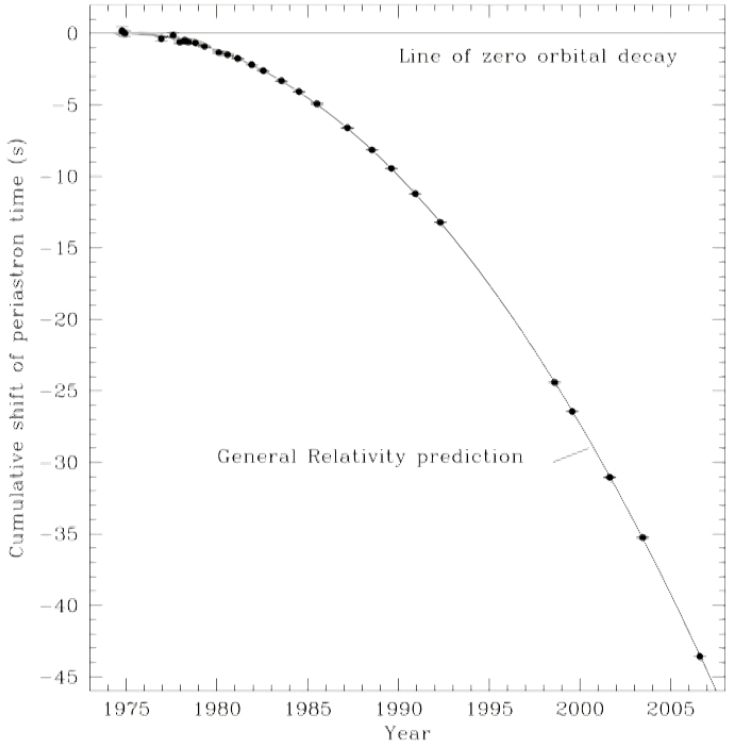

Table 3
Orbital Parameters

Parameter	Value[a]
T_0 (MJD)	52144.90097841(4)
$x \equiv a_1 \sin i$ (s)	2.341782(3)
e	0.6171334(5)
P_b (d)	0.322997448911(4)
ω_0 (deg)	292.54472(6)
$\langle\dot{\omega}\rangle$ (deg yr^{-1})	4.226598(5)
γ (ms)	4.2992(8)
$\dot{P}_b$	$-2.423(1) \times 10^{-12}$

Weisberg, Nice, Taylor, 2010, ApJ

Extra-dimension effect

RS model:

$$V = -\frac{GMm}{r}\left[1 + \frac{2}{3}\left(\frac{\ell}{GM}\right)^2\left(\frac{GM}{r}\right)^2 + \dots\right]$$

Emparan, Garcia-Bellido, Kaloper, 2003, JHEP

$$\frac{dM}{dt} = -2.8 \times 10^{-3} \left(\frac{M_\odot}{M}\right)^2 \left(\frac{L}{1\,\mathrm{mm}}\right)^2 M_\odot\,\mathrm{yr}^{-1}$$

In NS—BH system (Simonetti et al. 2011)

$$\dot{P}_{\mathrm{ML}} = -2P\frac{\dot{m}}{m} \quad >0$$

$$\chi^2 = \frac{\left(\left(\dot{P}_{\rm obs} - \Delta\dot{P}_{\rm gal}\right) - \left(\dot{P}_{\rm th}\right)\right)^2}{\sigma^2_{\dot{P}_{\rm obs}} + \sigma^2_{\Delta\dot{P}_{\rm gal}}}$$

Damour & Taylor (1991)

$$\Delta\dot{P}_{\rm b,gal} = -0.027 \pm 0.005 \times 10^{-12}$$

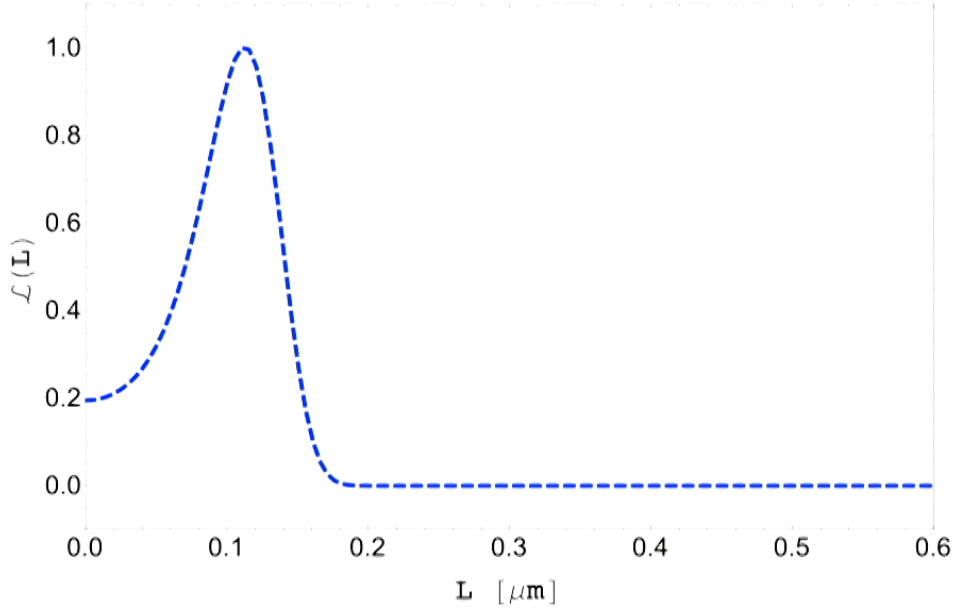

$L < 0.4\,\mu{\rm m}$ 99% confidence level

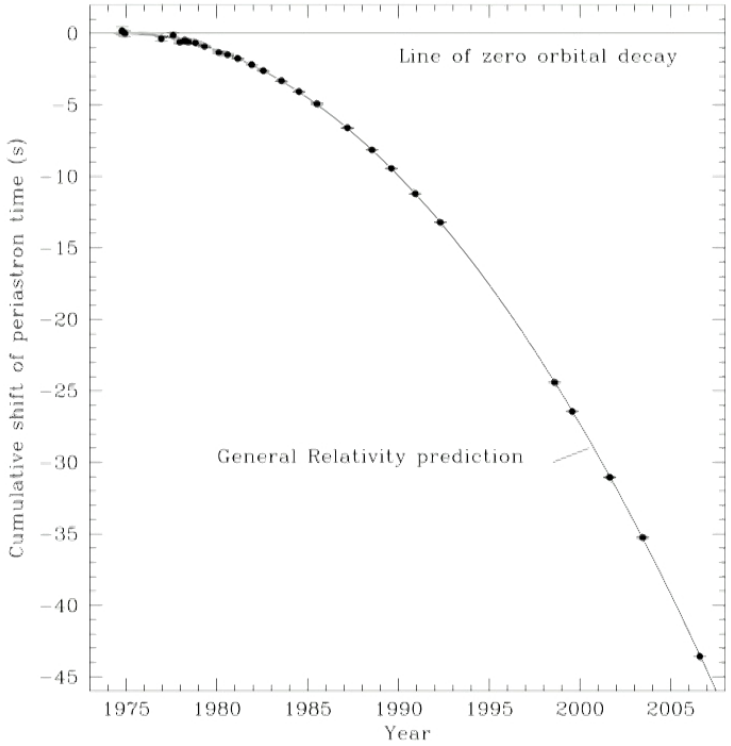

Table 3
Orbital Parameters

Parameter	Value[a]
T_0 (MJD)	52144.90097841(4)
$x \equiv a_1 \sin i$ (s)	2.341782(3)
e	0.6171334(5)
P_b (d)	0.322997448911(4)
ω_0 (deg)	292.54472(6)
$\langle\dot{\omega}\rangle$ (deg yr^{-1})	4.226598(5)
γ (ms)	4.2992(8)
$\dot{P}_b$	$-2.423(1) \times 10^{-12}$

Weisberg, Nice, Taylor, 2010, ApJ

$$\chi^2 = \frac{\left(\left(\dot{P}_{\rm obs} - \Delta\dot{P}_{\rm gal}\right) - \left(\dot{P}_{\rm th}\right)\right)^2}{\sigma^2_{\dot{P}_{\rm obs}} + \sigma^2_{\Delta\dot{P}_{\rm gal}}}$$

Damour & Taylor (1991)

$$\Delta\dot{P}_{\rm b,gal} = -0.027 \pm 0.005 \times 10^{-12}$$

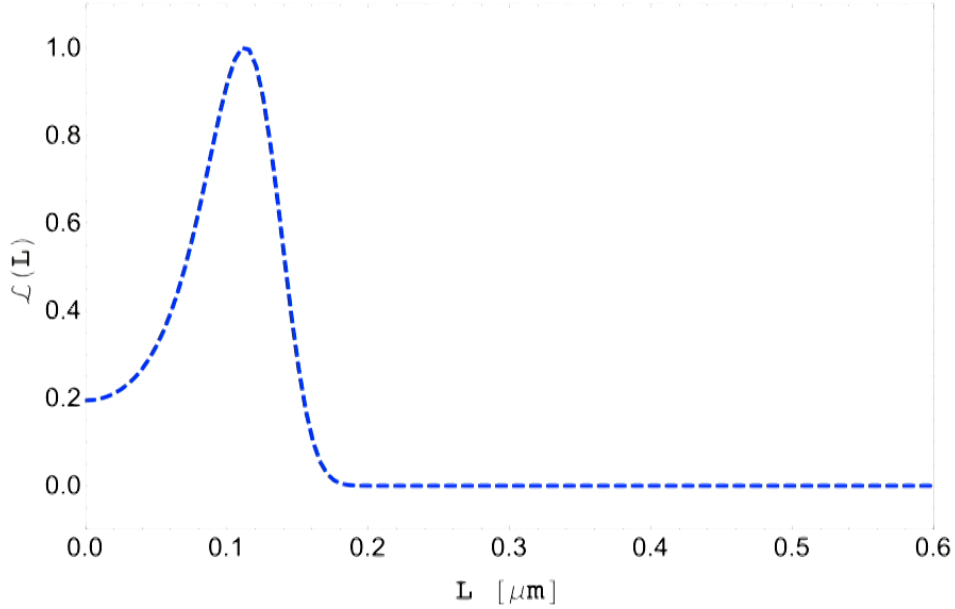

$L < 0.4\,\mu{\rm m}$ 99% confidence level

Theoretical Mechanism	GR Pillar	PN	$\lvert\beta\rvert$		Example Theory Constraints			
			GW150914	**GW151226**	Repr. Parameters	**GW150914**	**GW151226**	Current Bounds
Scalar Field Activation	SEP	-1	$\mathbf{1.6 \times 10^{-4}}$	$\mathbf{4.4 \times 10^{-5}}$	$\sqrt{\lvert\alpha_{\rm EdGB}\rvert}$ [km] $\lvert\dot{\phi}\rvert$ [1/sec]	—	—	10^{7} [56], 2 [57–59] 10^{-6} [60]
Scalar Field Activation	SEP, PI	$+2$	$\mathbf{1.3 \times 10^{1}}$	$\mathbf{4.1}$	$\sqrt{\lvert\alpha_{\rm dCS}\rvert}$ [km]	—	—	10^{8} [61, 62]
Vector Field Activation	SEP, LI	0	$\mathbf{7.2 \times 10^{-3}}$	$\mathbf{3.4 \times 10^{-3}}$	(c_+, c_-) $(\beta_{\rm KG}, \lambda_{\rm KG})$	$(\mathbf{0.9}, \mathbf{2.1})$ $(\mathbf{0.42}, -)$	$(\mathbf{0.8}, \mathbf{1.1})$ $(\mathbf{0.40}, -)$	$(0.03, 0.003)$ [63, 64] $(0.005, 0.1)$ [63, 64]
Extra Dimensions	4D	-4	$\mathbf{9.1 \times 10^{-9}}$	$\mathbf{9.1 \times 10^{-11}}$	ℓ [μm]	$\mathbf{5.4 \times 10^{10}}$	$\mathbf{2.0 \times 10^{9}}$	10–10^{3} [65–69]
Time-Varying G	SEP	-4	$\mathbf{9.1 \times 10^{-9}}$	$\mathbf{9.1 \times 10^{-11}}$	$\lvert\dot{G}\rvert$ [10^{-12}/yr]	$\mathbf{5.4 \times 10^{18}}$	$\mathbf{1.7 \times 10^{17}}$	0.1–1 [70–73]
Massive graviton	$m_g = 0$	$+1$	$\mathbf{1.3 \times 10^{-1}}$	$\mathbf{8.9 \times 10^{-2}}$	m_g [eV]	$\mathbf{10^{-22}}$ [19]	$\mathbf{10^{-22}}$ [5]	10^{-20}–10^{-18} [75–79]
Mod. Disp. Rel. (*Multifractional*)	LI	$+4.75$	$\mathbf{1.1 \times 10^{2}}$	$\mathbf{2.6 \times 10^{2}}$	E_*^{-1} [eV^{-1}] (time) E_+^{-1} [eV^{-1}] (space)	$\mathbf{5.8 \times 10^{-27}}$ $\mathbf{1.0 \times 10^{-26}}$	$\mathbf{3.3 \times 10^{-26}}$ $\mathbf{5.7 \times 10^{-26}}$	— 3.9×10^{-53} [80]
Mod. Disp. Rel. (*Modified Special Rel.*)	LI	$+5.5$	$\mathbf{1.4 \times 10^{2}}$	$\mathbf{4.3 \times 10^{2}}$	$\eta_{\rm dert}/L_{\rm Pl} > 0$ $\eta_{\rm dert}/L_{\rm Pl} < 0$	$\mathbf{1.3 \times 10^{22}}$	$\mathbf{3.8 \times 10^{22}}$	— 2.1×10^{-7} [80]
Mod. Disp. Rel. (*Extra Dim.*)	4D	$+7$	$\mathbf{5.3 \times 10^{2}}$	$\mathbf{2.4 \times 10^{3}}$	$\alpha_{\rm edt}/L_{\rm Pl}^2 > 0$ $\alpha_{\rm edt}/L_{\rm Pl}^2 < 0$	$\mathbf{5.5 \times 10^{62}}$	$\mathbf{2.5 \times 10^{63}}$	2.7×10^{2} [80] —
Mod. Disp. Rel. (*Standard Model Ext.*)	LI	$+4$	—	—	$\bar{k}_{(I)}^{(4)} > 0$ $\bar{k}_{(I)}^{(4)} < 0$	—	—	6.1×10^{-17} [80, 81] —
		$+5.5$	$\mathbf{1.4 \times 10^{2}}$	$\mathbf{4.3 \times 10^{2}}$	$\bar{k}_{(V)}^{(5)} > 0$ [cm] $\bar{k}_{(V)}^{(5)} < 0$ [cm]	$\mathbf{0.64}$ $\mathbf{1.7 \times 10^{-12}}$ [82]	$\mathbf{19}$ $\mathbf{3.1 \times 10^{-11}}$	— 1.7×10^{-40} [80, 81]
		$+7$	$\mathbf{5.3 \times 10^{2}}$	$\mathbf{2.4 \times 10^{3}}$	$\bar{k}_{(I)}^{(6)} > 0$ [cm^2] $\bar{k}_{(I)}^{(6)} < 0$ [cm^2]	$\mathbf{7.2 \times 10^{-4}}$	$\mathbf{3.3 \times 10^{-3}}$	— 3.5×10^{-64} [80, 81]
Mod. Disp. Rel. (*Hořava-Lifshitz*)	LI	$+7$	$\mathbf{5.3 \times 10^{2}}$	$\mathbf{2.4 \times 10^{3}}$	$\kappa_{\rm hl}^4 \mu_{\rm hl}^2$ [1/eV^2]	$\mathbf{1.5 \times 10^{6}}$	$\mathbf{6.9 \times 10^{6}}$	—
Mod. Disp. Rel. (*Lorentz Violation*)	LI	$+4$	—	—	c_+	$\mathbf{0.7}$ [83]	$\mathbf{0.998}$	0.03 [63, 64]

Yunes, Yagi, Pretorius, 2016, PRD

Theoretical Mechanism	GR Pillar	PN	$\lvert\beta\rvert$		Example Theory Constraints			
			GW150914	**GW151226**	Repr. Parameters	**GW150914**	**GW151226**	Current Bounds
Scalar Field Activation	SEP	-1	$\mathbf{1.6 \times 10^{-4}}$	$\mathbf{4.4 \times 10^{-5}}$	$\sqrt{\lvert\alpha_{\rm EdGB}\rvert}$ [km] $\lvert\dot{\phi}\rvert$ [1/sec]	—	—	10^{7} [56], 2 [57–59] 10^{-6} [60]
Scalar Field Activation	SEP, PI	$+2$	$\mathbf{1.3 \times 10^{1}}$	$\mathbf{4.1}$	$\sqrt{\lvert\alpha_{\rm dCS}\rvert}$ [km]	—	—	10^{8} [61, 62]
Vector Field Activation	SEP, LI	0	$\mathbf{7.2 \times 10^{-3}}$	$\mathbf{3.4 \times 10^{-3}}$	(c_+, c_-) $(\beta_{\rm KG}, \lambda_{\rm KG})$	$(\mathbf{0.9}, \mathbf{2.1})$ $(\mathbf{0.42}, -)$	$(\mathbf{0.8}, \mathbf{1.1})$ $(\mathbf{0.40}, -)$	$(0.03, 0.003)$ [63, 64] $(0.005, 0.1)$ [63, 64]
Extra Dimensions	4D	-4	$\mathbf{9.1 \times 10^{-9}}$	$\mathbf{9.1 \times 10^{-11}}$	ℓ [μm]	$\mathbf{5.4 \times 10^{10}}$	$\mathbf{2.0 \times 10^{9}}$	10–10^{3} [65–69]
Time-Varying G	SEP	-4	$\mathbf{9.1 \times 10^{-9}}$	$\mathbf{9.1 \times 10^{-11}}$	$\lvert\dot{G}\rvert$ [10^{-12}/yr]	$\mathbf{5.4 \times 10^{18}}$	$\mathbf{1.7 \times 10^{17}}$	0.1–1 [70–73]
Massive graviton	$m_g = 0$	$+1$	$\mathbf{1.3 \times 10^{-1}}$	$\mathbf{8.9 \times 10^{-2}}$	m_g [eV]	$\mathbf{10^{-22}}$ [19]	$\mathbf{10^{-22}}$ [5]	10^{-20}–10^{-18} [75–79]
Mod. Disp. Rel. (*Multifractional*)	LI	$+4.75$	$\mathbf{1.1 \times 10^{2}}$	$\mathbf{2.6 \times 10^{2}}$	E_*^{-1} [eV^{-1}] (time) E_+^{-1} [eV^{-1}] (space)	$\mathbf{5.8 \times 10^{-27}}$ $\mathbf{1.0 \times 10^{-26}}$	$\mathbf{3.3 \times 10^{-26}}$ $\mathbf{5.7 \times 10^{-26}}$	— 3.9×10^{-53} [80]
Mod. Disp. Rel. (*Modified Special Rel.*)	LI	$+5.5$	$\mathbf{1.4 \times 10^{2}}$	$\mathbf{4.3 \times 10^{2}}$	$\eta_{\rm dert}/L_{\rm Pl} > 0$ $\eta_{\rm dert}/L_{\rm Pl} < 0$	$\mathbf{1.3 \times 10^{22}}$	$\mathbf{3.8 \times 10^{22}}$	— 2.1×10^{-7} [80]
Mod. Disp. Rel. (*Extra Dim.*)	4D	$+7$	$\mathbf{5.3 \times 10^{2}}$	$\mathbf{2.4 \times 10^{3}}$	$\alpha_{\rm edt}/L_{\rm Pl}^2 > 0$ $\alpha_{\rm edt}/L_{\rm Pl}^2 < 0$	$\mathbf{5.5 \times 10^{62}}$	$\mathbf{2.5 \times 10^{63}}$	2.7×10^{2} [80] —
Mod. Disp. Rel. (*Standard Model Ext.*)	LI	$+4$	—	—	$\bar{k}_{(I)}^{(4)} > 0$ $\bar{k}_{(I)}^{(4)} < 0$	—	—	6.1×10^{-17} [80, 81] —
		$+5.5$	$\mathbf{1.4 \times 10^{2}}$	$\mathbf{4.3 \times 10^{2}}$	$\bar{k}_{(V)}^{(5)} > 0$ [cm] $\bar{k}_{(V)}^{(5)} < 0$ [cm]	$\mathbf{0.64}$ $\mathbf{1.7 \times 10^{-12}}$ [82]	$\mathbf{19}$ $\mathbf{3.1 \times 10^{-11}}$	— 1.7×10^{-40} [80, 81]
		$+7$	$\mathbf{5.3 \times 10^{2}}$	$\mathbf{2.4 \times 10^{3}}$	$\bar{k}_{(I)}^{(6)} > 0$ [cm^2] $\bar{k}_{(I)}^{(6)} < 0$ [cm^2]	$\mathbf{7.2 \times 10^{-4}}$	$\mathbf{3.3 \times 10^{-3}}$	— 3.5×10^{-64} [80, 81]
Mod. Disp. Rel. (*Hořava-Lifshitz*)	LI	$+7$	$\mathbf{5.3 \times 10^{2}}$	$\mathbf{2.4 \times 10^{3}}$	$\kappa_{\rm hl}^4 \mu_{\rm hl}^2$ [1/eV^2]	$\mathbf{1.5 \times 10^{6}}$	$\mathbf{6.9 \times 10^{6}}$	—
Mod. Disp. Rel. (*Lorentz Violation*)	LI	$+4$	—	—	c_+	$\mathbf{0.7}$ [83]	$\mathbf{0.998}$	0.03 [63, 64]

Yunes, Yagi, Pretorius, 2016, PRD

Black hole mining effect--- intersecting with cosmic string

Frolov and Fursaev, 2001, PRD

$$\dot{E} \simeq -\frac{1}{2400\pi}\frac{N_{\rm s}}{M^2}\left(\frac{c^6\hbar}{G^2}\right)$$

$$\Rightarrow \dot{M} = -\frac{1}{2400\pi}\frac{N_{\rm s}}{M^2}\left(\frac{c^4\hbar}{G^2}\right)$$

N*mu→ total back reaction, an order of one constant number

Therefore we have

$$\begin{aligned}\dot{M} &= -\frac{1}{4800\pi\tilde{\mu}}\frac{1}{M^2}\left(\frac{c^4\hbar}{G^2}\right) \\ &= -5.08\times10^{-60}\,\mu_7^{-1}\frac{1}{(M/{\rm M}_\odot)^2}\left(\frac{{\rm M}_\odot}{\rm yr}\right).\end{aligned}$$

Therefore

$$\dot{P}_{\rm MN} = 1.16\times10^{-62}\,P_{10}\mu_7^{-1}\,(M/{\rm M}_\odot)^{-3}$$

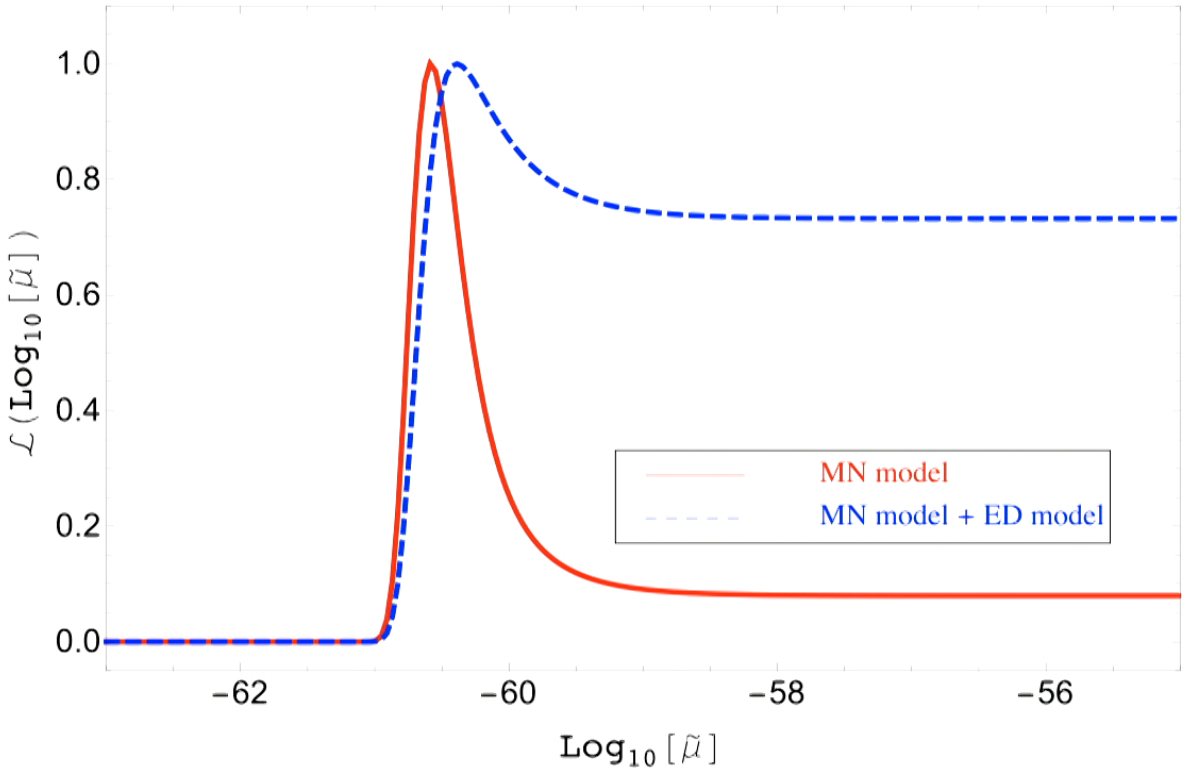

$$\log_{10}(\tilde{\mu}) > -61$$

Future data

Pulsar search

PSR--BH Binary system

Fast Radio Burst

MeerKAT/SKA telescope

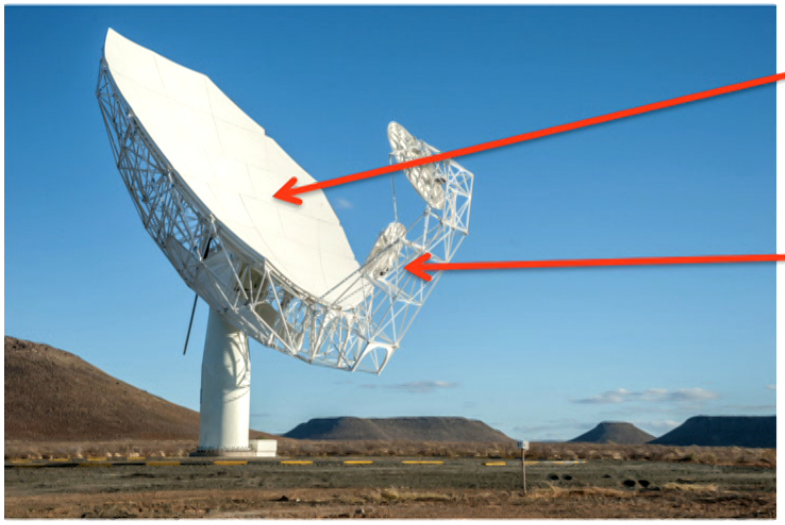

The antenna consists of the main reflector (effective diameter
13.5 m) plus the sub-reflector (diameter 3.8 m). The main reflector is made up of 40 panels, made of aluminum. The sub-reflector is a single composite structure.

- 64 antennas
- Sensitivity UHF band: 220m^2/K, L-band: 220→ 300 m^2/K, X-band: 200 m^2/K

MeerKAT/Square Kilometre Array

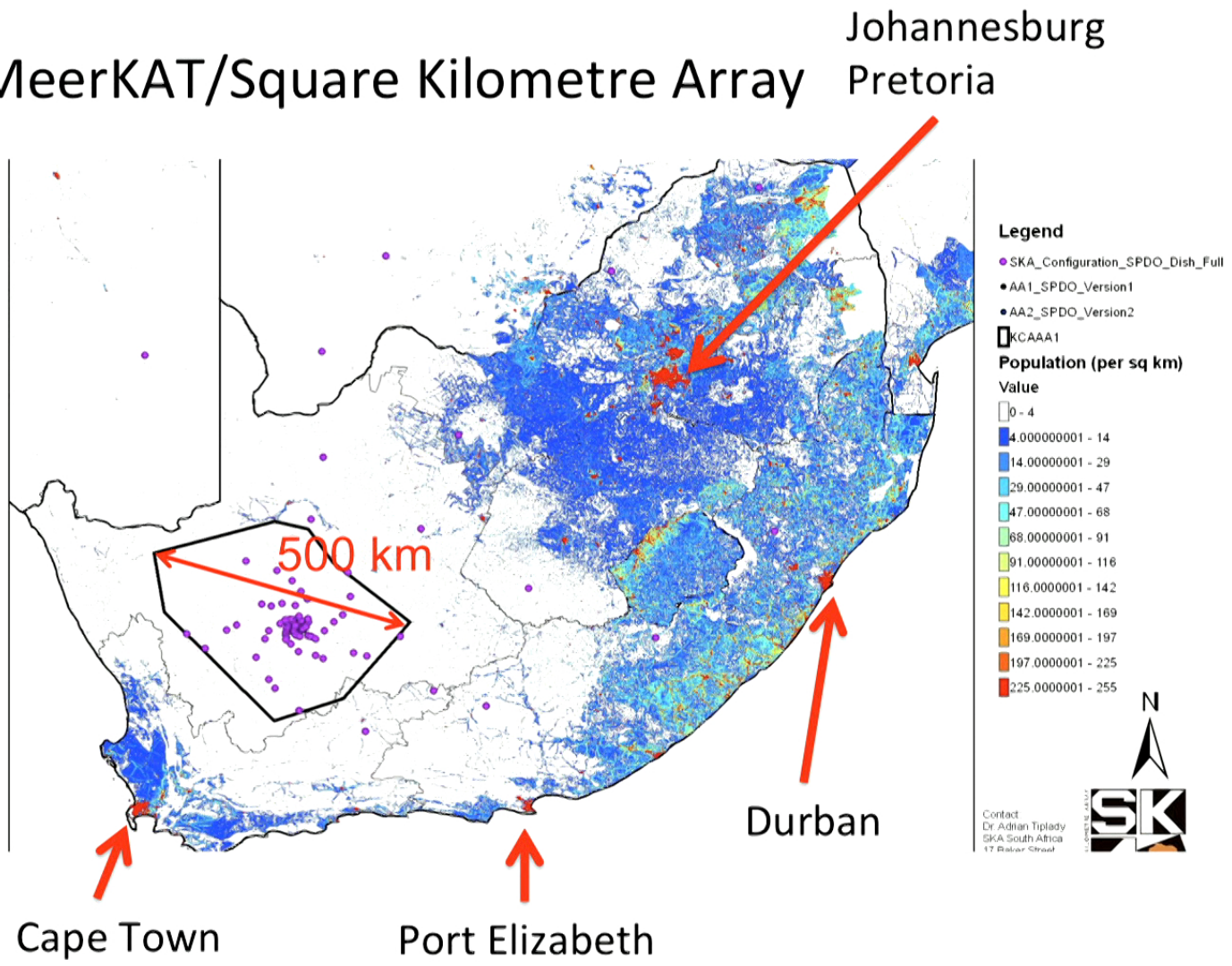

MeerKAT progress

- 16 receptors are installed by July 2016 (AR1) (each receptor consists of an antenna with receivers, digitizers and other electronics)
- AR2: 32 receptors by June 2017
- AR3: 64 receptors by April 2018

- LADUMA: Ultra-deep pencil beam HI survey [5000 h]
- MIGHTEE: MeerKAT international GigaHertz Tiered Extragalactic Exploration [2000 h]
- MHONGOOSE: MeerKAT HI Observations of Nearby Galactic Objects: Observing Southern Emitter
- VLBI: Extragalactic and local Universe survey
- TRAPUM: Transit and pulsar searches with MeerKAT [3000 h]
- ThunderKAT: The Hunt for Dynamic and Explosive Radio Transients with MeerKAT [3000h= 100 min/day for 5 years]
- Pulsar Timing
- MeerGAL: MeerKAT High Freqency Galactic Plane Survey [3300h]

MeerKAT progress

- 16 receptors are installed by July 2016 (AR1) (each receptor consists of an antenna with receivers, digitizers and other electronics)
- AR2: 32 receptors by June 2017
- AR3: 64 receptors by April 2018

- LADUMA: Ultra-deep pencil beam HI survey [5000 h]
- MIGHTEE: MeerKAT international GigaHertz Tiered Extragalactic Exploration [2000 h]
- MHONGOOSE: MeerKAT HI Observations of Nearby Galactic Objects: Observing Southern Emitter
- VLBI: Extragalactic and local Universe survey
- TRAPUM: Transit and pulsar searches with MeerKAT [3000 h]
- ThunderKAT: The Hunt for Dynamic and Explosive Radio Transients with MeerKAT [3000h= 100 min/day for 5 years]
- Pulsar Timing
- MeerGAL: MeerKAT High Freqency Galactic Plane Survey [3300h]

HIRAX: The Hydrogen Intensity and Real-time Analysis eXperiment

- UKZN/DUT/PI experiment on 21-cm IM and transiting objects

- 103 5-6m dishes, 400-800 MHz, 1024 channels.


Five-hundred-meter Aperture
Spherical Telescope - FAST
Guizhou Province

New pulsars have been discovered using FAST

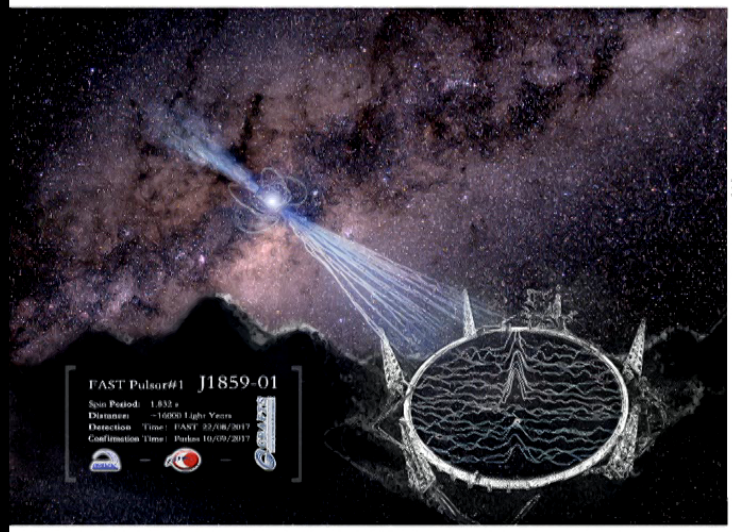

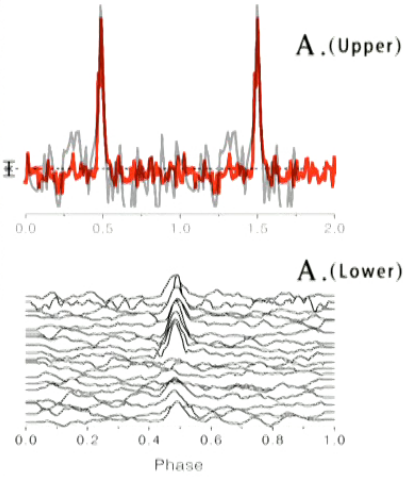

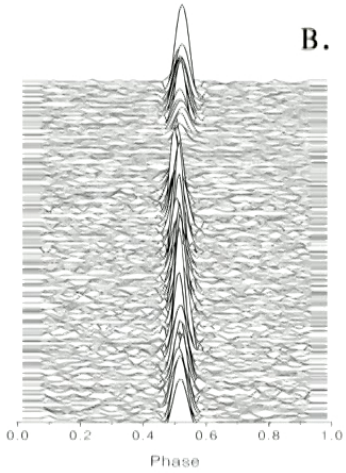

> **Two New pulsars have been discovered using FAST:** 10 Oct. 2017, a press conference to announce the first discoveries using FAST, two new pulsars were discovered in the Southern Galactic plane, i.e. PSR J1859-01 (FP1 or FAST pulsar #1), and PSR J1931-01 (FP2 or FAST pulsar #2). These two new pulsars have just been confirmed by the Parkes telescope in Australia.

> More than 10 new pulsars have been discovered up to now.

> For more details of pulsars discovered by FAST, please refer to http://crafts.bao.ac.cn/pulsar/ .

Summary:

1. Binary pulsars are the very accurate clock to test predictions of exotic physics. Extra-dimension, black hole mining effect can change the prediction of period changes.

2. We aim to obtain the tightest constraint on the size of extra-dimension. E.g. by using the PSR B1913+16, $L < 0.4\,\mu\mathrm{m}$, this is tighter than the GW150914 constraints.

3. We can also constrain the cosmic string density from BH mining effect, which gives a lower bound on the cosmic string tension.

4. Future radio astronomy survey will help to reveal more EM counterpart of the BH/NS merging event with <1 arcsec angular resolution. MeerKAT/SKA/HIRAX/ FAST will play a big role in providing more samples of the binary system, via direct imaging or interferometry.